

Simple Method for Numerical Simulation of Temperature Response of the Solid Rocket Nozzle

Timin Cai* and Xiao Hou†

Northwestern Polytechnical University, Xian, Shaanxi, China

This paper presents a simple method for numerical simulation of axisymmetric two-dimensional temperature distribution in a composite structure solid rocket nozzle. A body-fitted moving curvilinear coordinate system is adopted to deal with the complex contour of the nozzle and the moving boundary of ablation surface. The concept of equivalent volumetric heat capacity is also used to unify the energy balance equations of the control volume for all different material layers, which makes the moving boundaries caused by pyrolysis processes inside the material easy to handle. A time forward explicit scheme for the inner nodes and a time backward implicit scheme for the boundary nodes are used in numerical calculation. A sample calculation for an experimental solid rocket nozzle indicates that the numerical results of the temperature distribution agree with the measured data fairly well.

Nomenclature

A	= periphery area of control volume
c	= volumetric heat capacity
\bar{c}	= equivalent volumetric heat capacity
c_ϕ	= coefficient defined by Eq. (10)
g	= generalized heat conductivity
h_ϕ, h_z	= measure factor
ΔH	= heat of pyrolysis
ΔH_A	= heat of ablation
i, j	= grid-point index in ϕ and z directions, respectively
k	= heat conductivity
$L(z)$	= radius of backside contour of the nozzle
\dot{m}_w	= total ablation rate of the material
M, N	= grid-point number in ϕ and z directions, respectively
\bar{n}	= outward normal unit vector of dA
q_ϕ, q_z	= generalized heat flux in ϕ and z directions, respectively
\bar{q}	= heat flux vector
q_c	= convective heat flux
q_r	= net radiative heat flux
r, θ, z	= cylindrical coordinates
$R(z, \tau)$	= radius of inner wall of the nozzle
T	= temperature
V	= total volume of the control volume
x, y, z	= rectangular coordinates
τ	= time
ρ	= density of the material
ϕ	= transformed radial coordinate
ψ	= blowing factor
$\dot{\omega}$	= pyrolysis rate

Subscripts

e	= ending point of the pyrolysis processes
l	= lower (or right) side node of the interface
o	= initial time
s	= starting point of the pyrolysis processes
u	= upper (or left) side node of the interface
1	= char layer

2	= pyrolysis layer
3	= virgin material layer
4	= zone of the throat lining

Introduction

WITH the increase of the energy of solid composite propellant, the thermal protection problem must be well treated in the nozzle structure design. For this reason, different kinds of composite materials with low density, low conductivity, low ablation rate, and high thermostrength are used in solid rocket nozzles. For a composite structure nozzle, uncharring carbon-based composite materials such as graphite and carbon-carbon are often used for the throat lining, and charring composite materials such as silica- and carbon-phenolics are used for the convergent, divergent section of the nozzle and the back lining of the throat part. This kind of nozzle is usually of complex contour. During firing, the inner wall surface of the nozzle recedes due to the chemical-thermo ablation and the mechanical ablation under the action of the gas, which is of high temperature and high velocity. In the meantime, pyrolysis processes take place inside the charring composite material, which causes the interfaces between the virgin material layer and the pyrolysis layer, and the pyrolysis layer and the char layer, to move continuously, so that it is very difficult to calculate the temperature distribution of the composite structure nozzle, and some simplifications must be made. The simplest method is a one-dimensional calculation that uses the relative coordinate system to tackle the moving boundary, and the temperature in the virgin material, pyrolysis, and char layers is calculated, respectively. In this method, if a pyrolysis surface model is assumed, the temperature at the pyrolysis surface is set to be the ending point of pyrolysis temperature.¹ If a pyrolysis layer model that is better than the pyrolysis surface model is used, the pyrolysis processes are completed in a certain layer corresponding to the pyrolysis temperature range of the material.^{2,3} For the two-dimensional case, the temperature calculation is more complicated. The finite-difference method based on the orthogonal mesh system and the principle of energy balance applied to the control volumes is only applicable to the temperature field calculation of the uncharring carbon-based composite material nozzle using a cell-dropping technique to tackle the ablative moving boundary.⁴ Zedan and Schneider have discussed the application of an energy balance to the control volumes in a nonorthogonal coordinate system, but the variation of material properties and moving boundary are not considered.⁵ Zhenzhong⁶ has used the moving coordinate system, which is

Received Dec. 8, 1987; revision received Jan. 8, 1988; presented as Paper 88-0083 at the AIAA 26th Aerospace Sciences Meeting, Reno, NV, Jan. 11-14, 1988. Copyright © 1989 American Institute of Aeronautics and Astronautics, Inc. All rights reserved.

*Professor, Head, Department of Astronautical Engineering.

†Graduate Student, Ph.D. candidate.

coordinated with the ablative boundary, to calculate the temperature field for atmospheric entry, but it is also available only for uncharring carbon-based composite materials.

If a composite structure nozzle consists of both uncharring carbon-based composite material and charring composite material, then not only the ablative moving boundary at the inner wall but also the moving boundaries of the pyrolysis layer inside the material need to be treated. The latter are also curves in the transformed plane that will bring great difficulties in temperature field calculation. The purpose of this paper is to offer a simple method that can easily tackle these two kinds of moving boundaries for calculating the temperature field of an entire composite structure nozzle. In this paper a coordinate transformation method is used to change the fixed rectangular coordinate system into a body-fitted curvilinear moving coordinate system and to change the complex geometry with moving boundary into a fixed rectangular computational domain. For the moving boundaries of the pyrolysis layer inside the material, the concept of an equivalent volumetric heat capacity is introduced⁷ so that the source term of heat absorption due to pyrolysis in the energy balance equation of control volume can be converted into an equivalent volumetric heat capacity. The energy balance equations for control volumes in all different material layers may then be unified, provided that corresponding material property parameters are provided for them. In this case it is not necessary to calculate each layer respectively. After solving the temperature field, the thickness of the pyrolysis and char layers can be determined according to the starting and ending points of the pyrolysis temperature range.

Unified Energy Balance Equation

As mentioned previously, when a solid rocket motor is firing, the inner wall surface of the nozzle recedes due to ablation, and the charring composite material will form three layers, i.e., the virgin material, pyrolysis, and char layers, as shown in Fig. 1. Assuming that the secondary decomposition of pyrolysis gas doesn't appear and that the cooling effect caused by outflow of the pyrolysis gas is negligible, we can write unified energy balance equations for the control volume of all different material layers as follows

$$-\int_V c_i \frac{\partial T}{\partial \tau} dv = \int_A \bar{q} \cdot \bar{n} dA \quad i = 1, 2, 3, 4 \quad (1)$$

For the pyrolysis layer, c_2 is the equivalent volumetric heat capacity, and its expression is deduced as follows: The energy balance equation for the control volumes in the pyrolysis layer should be

$$-\int_V c_2' \frac{\partial T}{\partial \tau} dv = \int_A \bar{q} \cdot \bar{n} dA + \int_V \dot{\omega} \Delta H dv \quad (2)$$

where c_2' is the volumetric heat capacity of the pyrolysis layer.

The results of mass loss experiments for the silica-phenolics show that the relationship between mass loss and temperature is approximately linear for the pyrolysis layer. In fact, Nelson

has shown this relationship previously.⁸ Therefore, we may write

$$\rho_2 = \rho_3 - \frac{\rho_3 - \rho_1}{T_e - T_s} (T - T_s) \quad (3)$$

Assuming that the volume of the material remains constant during the pyrolysis processes, we have

$$\dot{\omega} = -\frac{d\rho_2}{d\tau} = \frac{\rho_3 - \rho_1}{T_e - T_s} \cdot \frac{\partial T}{\partial \tau} \quad (4)$$

Substituting Eq. (4) into Eq. (2) and recombining, we get

$$-\int_V c_2 \frac{\partial T}{\partial \tau} dv = \int_A \bar{q} \cdot \bar{n} dA$$

This is the same form as Eq. (1), where

$$c = c_2' + \frac{\rho_3 - \rho_1}{T_e - T_s} \cdot \Delta H \quad (5)$$

Coordinate System Transformation

To tackle the ablative moving boundary, the fixed rectangular coordinate system is transformed into a body-fitted curvilinear moving coordinate system. Then the complex nozzle geometry with moving boundary is changed into a fixed rectangular computational domain. Although the energy balance equation for the control volumes will become more complicated, it allows us to deal only with fixed boundary and to use equally spaced mesh, making the finite-difference calculation more convenient. Since the nozzle is axisymmetric, the cylindrical coordinate system (r, θ, z) is preferable to the rectangular coordinate system (x, y, z), as shown in Fig. 2.

By extension of the Landau transformation to the two-dimensional case, radial coordinate r is further transformed into ϕ .^{9,10} The transformation expression is

$$\phi = \frac{r - R(z, \tau)}{L(z) - R(z, \tau)} \quad (6)$$

Here we assume that $\partial R / \partial z$ exists even during ablation. From Eq. (6) we have

$$r = R(z, \tau), \quad \phi = 0$$

$$r = L(z) \quad \phi = 1$$

For the axisymmetric two-dimensional case, $\partial T / \partial \theta = 0$; taking $\Delta \theta = 1$, temperature is calculated only in a computational plane consisting of axis ϕ and axis z , shown in Fig. 3, where H is the length of the nozzle.

In the $\phi - z$ plane the rectangular domain is divided into meshes by horizontal and vertical lines. For each inner node in the $\phi - z$ plane we take a control area, as shown in Fig. 4.

Now we write its energy balance equation, which is trans-

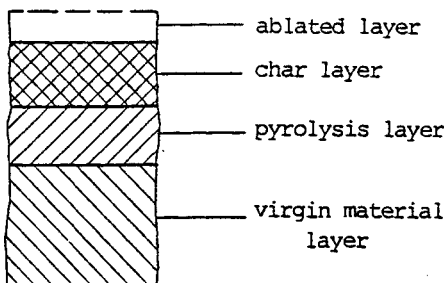


Fig. 1 Ablation model of the charring composite material.

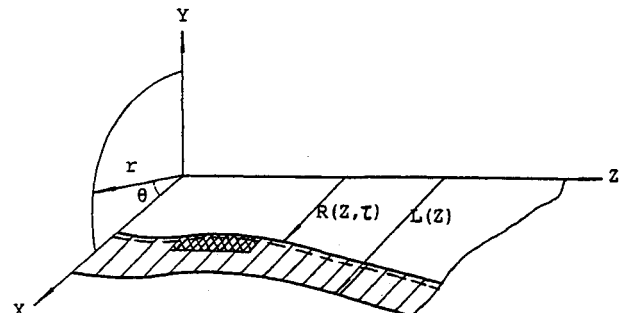


Fig. 2 Coordinate systems for the nozzle.

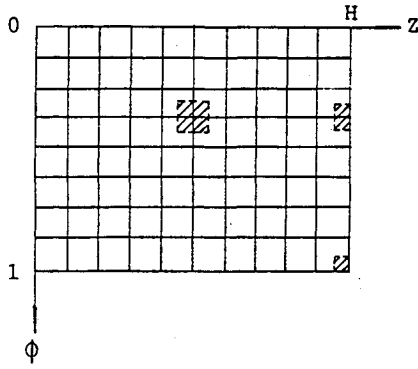


Fig. 3 Computational plane.

formed from Eq. (1):

$$\begin{aligned} & \left[\bar{c}r \left(L - R \right) \left(\frac{\partial T}{\partial \tau} - \frac{1 - \phi}{L - R} \frac{\partial R}{\partial \tau} \frac{\partial T}{\partial \phi} \right) \right]_{i,j} \cdot \Delta \phi \Delta z \\ &= (q_{\phi} r \sqrt{1 + c_{\phi}^2})_{i-1/2,j} \cdot \Delta Z - (q_{\phi} r \sqrt{1 + c_{\phi}^2})_{i+1/2,j} \cdot \Delta z \\ &+ [q_z r (L - R)]_{i,j-1/2} \cdot \Delta \phi - [q_z r (L - R)]_{i,j+1/2} \cdot \Delta \phi \quad (7) \end{aligned}$$

where

$$\bar{c} = c \left(1 + \frac{T}{C} \frac{\partial C}{\partial T} \right) \quad (8)$$

$$\frac{\partial R}{\partial \tau} = \frac{\dot{m}_w}{\rho_1} \sqrt{1 + \left(\frac{\partial R}{\partial z} \right)^2} \quad (9)$$

$$c_{\phi} = (1 - \phi) \frac{\partial R}{\partial z} + \phi \frac{dL}{dz} \quad (10)$$

$$\begin{pmatrix} q_{\phi} \\ q_z \end{pmatrix} = - \begin{pmatrix} g_{\phi\phi} & g_{\phi z} \\ g_{z\phi} & g_{zz} \end{pmatrix} \begin{pmatrix} \frac{1}{h_{\phi}} \frac{\partial T}{\partial \phi} \\ \frac{1}{h_z} \frac{\partial T}{\partial z} \end{pmatrix} \quad (11)$$

$$h_{\phi} = \frac{L - R}{\sqrt{1 + C_{\phi}^2}}, \quad h_z = 1 \quad (12)$$

$$g_{\phi\phi} = \frac{1}{1 + C_{\phi}^2} (k_r + C_{\phi}^2 k_z)$$

$$g_{\phi z} = g_{z\phi} = - \frac{C_{\phi}}{\sqrt{1 + C_{\phi}^2}} \cdot k_z \quad (13)$$

$$g_{zz} = k_z$$

here, $\partial R / \partial \tau$ is the recession rate of inner wall due to ablation. From Eq. (9) it is seen that the calculation of total ablation rate of the material must be coupled with the temperature field calculation at each time step. However, this is not covered in this paper. In calculation, the experimentally measured average recession rate of the inner wall is used.

Numerical Method

Substituting Eqs. (8–13) into Eq. (7) and using a forward explicit scheme for the time derivative and a central difference scheme for the space derivatives, a series of difference equations for the inner nodes can be derived to solve the temperature at all inner nodes directly. A backward implicit scheme

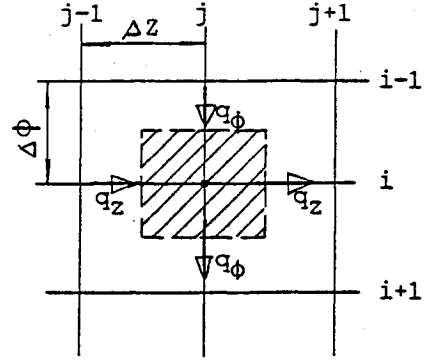


Fig. 4 Control area in the mesh.

for the time derivative and a second-order forward or backward difference scheme for the space derivatives are used to derive the difference equations for the boundary nodes, which will improve the numerical stability. Joining with the boundary conditions we can get a system of tridiagonal algebraic equations that is quite easy to solve.

The initial condition and boundary conditions are given as follows:

$$\tau = 0, \quad T_{i,j} = T_0 \quad 1 \leq i \leq M, \quad 1 \leq j \leq N$$

$$z = H, \quad (q_z)_{i,N} = 0$$

$$z = 0, \quad (q_z)_{i,1} = 0, \quad 2 \leq i \leq M - 1$$

$$\phi = 1, \quad (q_{\phi})_{M,j} = 0$$

$$\phi = 0, \quad (q_{\phi})_{1,j} = \psi q_c + q_r - \dot{m}_w H_A, \quad 1 \leq j \leq N$$

Here, the conductive heat flux is calculated by the semiempirical Bartz relations.^{11,12} The net radiative heat flux is calculated by the parallel grey plates model.

In calculation, the variable property parameters of material are used, and the anisotropy is also considered. The specific heat and conductivity are assumed to be of linear relationship with the temperature in the pyrolysis layer.³ At the interfaces between the two different layers of quite different heat conductivities, such as graphite throat lining/charring material nozzle, and char layer/pyrolysis layer, it is better to determine the heat conductivity by the following expression¹³:

$$k = \frac{2k_u k_l}{k_u + k_l} \quad (14)$$

Since the property parameters of the material vary with the temperature, the system of difference equations for the boundary nodes is of some nonlinearity. It is necessary to solve the temperature iteratively at each time step, but usually two or three iterations are enough to obtain satisfactory accuracy.

If the temperature at each time step has been solved, the moving interfaces inside the charring composite material, i.e., the thickness of the char and pyrolysis layers, can easily be determined by the following criteria:

$$T_{i,j} < T_s \quad \text{virgin material layer}$$

$$T_s < T_{i,j} < T_e \quad \text{pyrolysis layer}$$

$$T_{i,j} < T_e \quad \text{char layer}$$

Computation Sample and Experiment

Temperature field calculation for a small experimental solid rocket nozzle has been carried out by the method described.

Graphite throat lining is used for the experimental rocket nozzle, and the convergent and divergent sections of the nozzle and the back lining of the throat part are made of silica-phenolics. The diameter of the throat part is 11 mm, the diameter of exit section of the nozzle is 27 mm, the divergence angle is 20 deg, the length of entire nozzle H is 75 mm, and the radius of the backside contour of the nozzle $L(z)$ is 33 mm (constant along axis z). The composite propellant contains 14% aluminum powder. The combustion temperature is 3462 K, and the operating pressure is 4.41 MPa. The time duration is 24 s. During firing, the temperature field of a section in the divergent part with $z = 51$ mm and initial radius $R = 9.2$ mm is measured by Pt-Rh₁₀-Pt thermocouple. The precise location of the three thermocouples are

$$z = 51 \text{ mm}, \quad r_1 = 12.08 \text{ mm}, \quad r_2 = 13 \text{ mm}, \quad r_3 = 15.95 \text{ mm}$$

The calculation covers an area from the left side of the throat lining to the exit section of the nozzle, and a grid point of 15×16 is used. In calculation, we take

$$T_o = 278 \text{ K}, \quad T_s = 600 \text{ K}, \quad T_e = 950 \text{ K}$$

The value of equivalent surface emissivity for the parallel grey plates model is $0.8548 \cdot 10^{-8} \text{ W/M}^2\text{K}^4$, and the experimentally measured average recession rate of inner wall used in calculation is about 0.03 mm/s.

The thermophysical properties of the materials used in this computation sample are listed as follows:

Silica-phenolics virgin material:

$$K_3 = 0.372 \text{ W/Mk}$$

$$C_3 = 1765 \text{ kg/M}^3 \cdot 1.382 \text{ kJ/kg k} = 2439.2 \text{ kJ/M}^3\text{k}$$

Char layer of silica-phenolics:

$$K_1 = 2.1 \text{ W/Mk}$$

$$C_1 = 1360 \text{ kg/M}^3 \cdot 1.13 \text{ kJ/kg k} = 1536.8 \text{ kJ/M}^3\text{k}$$

Graphite:

$$(K_4)_z = 248.834 - 181.086 \cdot 10^{-3}T + 40.306$$

$$\cdot 10^{-6}T^2 \text{ W/Mk}$$

$$(K_4)_z = 311.396 - 274.56 \cdot 10^{-3}T + 69.406$$

$$\cdot 10^{-6}T^2 \text{ W/Mk}$$

$$C_4 = 1825 \text{ kg/M}^3 \cdot (-77.665 + 2105.96 \cdot 10^{-3}T - 509.115 \cdot 10^{-6}T^2) \text{ J/kg k} = -141.738 + 3.843T - 0.929 \cdot 10^{-3}T^2 \text{ kJ/M}^3\text{k}$$

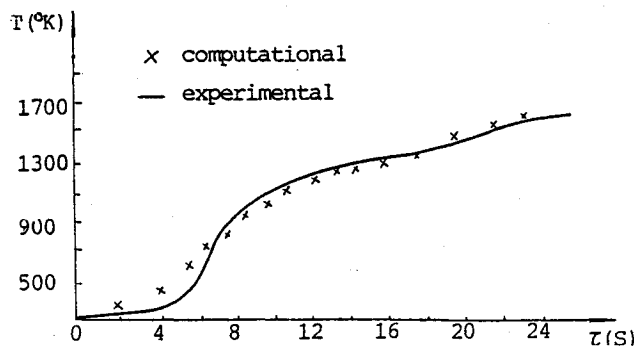


Fig. 5 Temperature history at a measuring point of the nozzle.

The computational and experimental results are shown in Figs. 5-7.

Figure 5 shows the computational and experimental temperatures of a measuring point at the divergent section of the nozzle ($z = 51$ mm, $r_2 = 13$ mm, i.e., with a depth of 3.8 mm) varying with the time. From the curves we can see that the results are quite consistent. The relative error is less than 13% from $\tau = 6.5$ to 24 s. But the discrepancy is obvious prior to $\tau = 6.5$ s. The lack of coupling with ablation rate calculation may be one of the causes. The approximate treatment of the pyrolysis zone could also be a contributing cause. Besides, the uniform mesh used in the sample may also induce certain errors, especially in the near inner wall area, where the temperature gradient is quite large.

Figure 6 shows the computed inner wall temperature distribution along the z axis at three different time levels; nodes 2-9 subject to the location of graphite throat lining, nodes 9-16 subject to the location of the silica-phenolics divergent part of the nozzle, and node 7 subject to the location of the throat part. From the curves we can see that there is a peak of inner wall temperature at the throat part since the heat flux there is of highest value. There is another peak of inner wall temperature that is even higher than the first one at node 11, because the heat conductivity of silica-phenolics is much lower than the heat conductivity of graphite.

Figure 7 shows the computational and experimental char layer front distribution along the z axis at the end of firing, i.e., $\tau = 24$ s. From the curves we can see that these results are also quite consistent.

Conclusion

A body-fitted curvilinear moving coordinate system and the concept of equivalent volumetric heat capacity can simplify the method of tackling the ablative moving boundary and the pyrolysis moving boundaries in the numerical simulation of the temperature response of solid rocket nozzles. This method may be applied to axisymmetric two-dimensional temperature field calculation for the entire composite structure nozzle independent of how many kinds of composite materials are used,

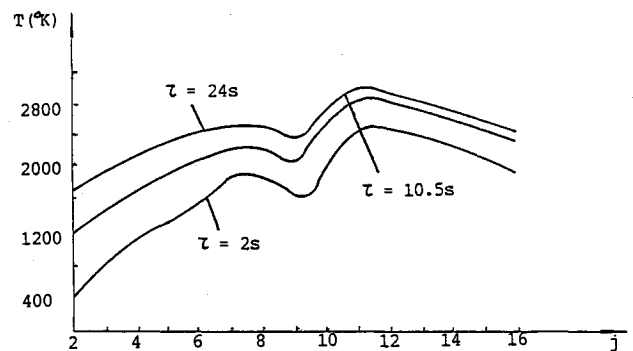


Fig. 6 Inner wall temperature distribution along z axis.

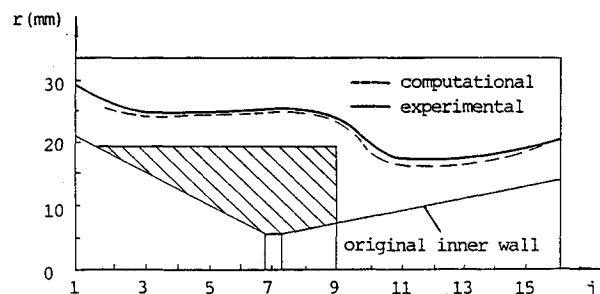


Fig. 7 Char layer front distribution along z axis.

and the computational results are accurate enough for engineering design purposes. However, some work remains to be done to improve the accuracy further, such as coupling the temperature calculation with the ablation rate calculation, finding a better technique of grid generation, etc.

References

- ¹Swann, R. T. and Pittman, C. M., "Numerical Analysis of the Transient Response of Advanced Thermal Protection System for Atmospheric Entry," NASA TN D-1370, July 1962.
- ²Matting, F. W., "Analysis of Charring Ablation with Description of Associated Computing Program," NASA TN D-6085, Nov. 1970.
- ³Jiang, G. Q., "An Integral Method for Calculation of Heat Conduction with Mass Transfer and Chemical Reaction," *Journal of the Chinese Society of Astronautics*, No. 1, 1980, pp. 50-59.
- ⁴Schoner, R. J., Schaefer, J. W., and Wool, M. R., "Aerotherm Axisymmetric Transient Heating and Material Ablation Computer Program (ASTHMA)," AD-744853, Vol. I, 1972.
- ⁵Zedan, M. and Schneider, G. E., "A Physical Approach to the Finite-Difference Solution of the Conduction Equation in Generalized Coordinates," *Numerical Heat Transfer*, Vol. 5, 1982, pp. 1-19.
- ⁶Huang, Z. Z., "A Comprehensive Analysis Algorithm for Ablation, Temperature Field and Thermal Stresses of the Carbon-Based Nosetips," *Journal of the Chinese Society of Astronautics*, No. 3, 1984, pp. 30-38.
- ⁷Bonacina, C., Comini, G., Fasano, A., and Primicerio, M., "Numerical Solution of the Phase-Change Problems," *International Journal of Heat and Mass Transfer*, Vol. 16, No. 10, Oct. 1973, pp. 1825-1832.
- ⁸Nelson, J. B., "Determination of Kinetic Parameters of Six Ablation Polymers by Thermogravimetric Analysis," NASA TN D-3919, April 1967.
- ⁹Spaid, F. W., Charwat, A. F., Redekopp, L. G., and Rosen, R., "Shape Evolution of a Subliming Surface Subjected to Unsteady Spatially Nonuniform Heat Flux," *International Journal of Heat and Mass Transfer*, Vol. 14, No. 5, May 1971, pp. 673-687.
- ¹⁰Duda, J. L., Malone, M. F., Notter, R. H., and Vientas, J. S., "Analysis of Two-Dimensional Diffusion-Controlled Moving Boundary Problems," *International Journal of Heat and Mass Transfer*, Vol. 18, No. 7/8, 1975, pp. 901-910.
- ¹¹Bartz, D. R., "Turbulent Boundary Layer Heat Transfer from Rapidly Accelerating Flow of Rocket Combustion Gases and of Heated Air," Jet Propulsion Laboratory TR 32-387, 1965.
- ¹²Godai, T. and Yuzawa, Y., "An Experimental Investigation of Heat Transfer in the Nozzle of High-Aluminized Solid Rocket," NASA-TT-F-12106, 1968.
- ¹³Patankar, S. V., *Numerical Heat Transfer and Fluid Flow*, McGraw-Hill, New York, 1980, pp. 44-47.

*Recommended Reading from the AIAA
Progress in Astronautics and Aeronautics Series . . .*



Opportunities for Academic Research in a Low-Gravity Environment

George A. Hazelrigg and Joseph M. Reynolds, editors

The space environment provides unique characteristics for the conduct of scientific and engineering research. This text covers research in low-gravity environments and in vacuum down to 10^{-15} Torr; high resolution measurements of critical phenomena such as the lambda transition in helium; tests for the equivalence principle between gravitational and inertial mass; techniques for growing crystals in space—melt, float-zone, solution, and vapor growth—such as electro-optical and biological (protein) crystals; metals and alloys in low gravity; levitation methods and containerless processing in low gravity, including flame propagation and extinction, radiative ignition, and heterogeneous processing in auto-ignition; and the disciplines of fluid dynamics, over a wide range of topics—transport phenomena, large-scale fluid dynamic modeling, and surface-tension phenomena. Addressed mainly to research engineers and applied scientists, the book advances new ideas for scientific research, and it reviews facilities and current tests.

TO ORDER: Write, Phone, or FAX: AIAA Order Department,
370 L'Enfant Promenade, S.W., Washington, DC 20024-2518
Phone (202) 646-7444 ■ FAX (202) 646-7508

Sales Tax: CA residents, 7%; DC, 6%. Add \$4.50 for shipping and handling.
Orders under \$50.00 must be prepaid. Foreign orders must be prepaid.
Please allow 4 weeks for delivery. Prices are subject to change without notice.
Returns will be accepted within 15 days.

1986 340 pp., illus. Hardback
ISBN 0-930403-18-5
AIAA Members \$59.95
Nonmembers \$84.95
Order Number V-108